






Instantaneous areal population density of entire Atlantic cod and herring spawning groups and group size distribution relative to total spawning population

Nicholas C. Makris¹  | Olav Rune Godø^{2,3}  | Dong Hoon Yi¹ |
 Gavin J. Macaulay²  | Ankita D. Jain¹ | Byunggu Cho¹  | Zheng Gong¹ |
 Josef Michael Jech⁴  | Purnima Ratilal⁵

¹Center for Ocean Engineering, Massachusetts Institute of Technology, Cambridge, Massachusetts

²Institute of Marine Research, Bergen, Norway

³Christian Michelsen Research, Bergen, Norway

⁴NOAA Northeast Fisheries Science Center, Woods Hole, Massachusetts

⁵Department of Electrical and Computer Engineering, Northeastern University, Boston, Massachusetts

Correspondence

Nicholas C. Makris, Center for Ocean Engineering, Massachusetts Institute of Technology, Cambridge, MA.
 Email: makris@mit.edu

Funding information

Norwegian Institute of Marine Research (IMR); Office of Naval Research (ONR); National Science Foundation (NSF)

Abstract

The wide-area group behaviour of spawning Atlantic cod and herring is investigated. By a combination of Ocean Acoustic Waveguide Remote Sensing (OAWRS) and conventional sensing methods, first-look images of the instantaneous population density are obtained of entire Atlantic cod spawning groups, stretching for tens of kilometres in the Nordic Seas. This structural information made it possible to quantify the spawning group size distribution of cod over a roughly 30-year period from conventional line-transect data acquired annually by vertical echo sounding in the Nordic Seas. The size distribution is found to be consistent with the log-normal probability density often found in growth processes that depend on many independent parameters. Nordic Seas cod populations are found to distribute into many vast behavioural groups during spawning with relatively stable mean size despite larger variations in total annual population. When sustained at pre-industrial levels, the total spawning population is found to greatly exceed the mean spawning group size. As an apparent consequence of this large differential, when the total population, or overall scale, declined to within a standard deviation of this mean cod spawning group quantum, or inner-group-behavioural scale, return to pre-industrial levels required decades. Findings for Atlantic herring are similar, where summing the spawning group populations measured in a single instantaneous OAWRS image per day over the 8-day peak spawning period enabled accurate enumeration of the entire Georges Bank herring spawning population to within 7% of the independent NOAA estimate for 2006. These results may be relevant to other oceanic fish.

KEYWORDS

ecosystem sensing, fish group behaviour, fish shoal, Ocean Acoustic Waveguide Remote Sensing, oceanic fish sustainability, population collapse and recovery

1 | INTRODUCTION

Oceanic fish groups occupy vast undersea areas that are difficult to sample without significant aliasing in space and time with conventional survey methods (Berdahl, Westley, Levin, Couzin, & Quinn, 2016; Klemas, 2013; Ritz, Hobday, Montgomery, & Ward, 2011; Stock et al., 2011). This has often made it challenging to study the natural group behavioural processes of many oceanic fish populations and how they relate to industrial-age population variations and declines (Croft, Krause, Couzin, & Pitcher, 2003; Koslow, 2009; Mackinson, Sumaila, & Pitcher, 1997; Nicol & Brierley, 2010; Pitcher, Hart, & Pauly, 2012; Rose, 2007). The most abundant oceanic fish species are known to gather in immense groups during spawning (Pitcher, 1986; Rose, 1993), where the term “fish groups” as used here follows the definition of “fish shoals” as “groups of fish which remain together for social reasons” (Pitcher, 1986). Here, we use ocean acoustic waveguide remote sensing (OAWRS), which provides instantaneous continental-shelf-scale population density imagery (Jagannathan et al., 2009; Makris et al., 2006, 2009), in conjunction with conventional methods to investigate group behaviour of Atlantic cod (*Gadus morhua*) in the Nordic Seas during the main spawning periods.

We present first-look images of the instantaneous population density of entire Atlantic cod spawning groups, stretching for tens of kilometres in the Nordic Seas. With the aid of group morphology revealed by OAWRS, we provide a multi-decadal quantification of the spawning group size distribution of Atlantic cod in the Nordic Seas from conventional acoustic survey and catch data. We then compare mean group size to total spawning population size over time. To put the results in broader perspective, similar analysis is performed for Atlantic herring (*Clupea harengus*), where OAWRS data also have made it possible to quantify entire spawning groups (Makris et al., 2009; Wang et al., 2016; Yi, Gong, Jech, Ratilal, & Makris, 2018). Quantification of the instantaneous horizontal morphologies of entire spawning groups has currently been achieved for only two species and so the study is limited to these two, where the relevant measurements were made with OAWRS. Without such ground truth observations of group morphology for a given species, it is difficult or impossible to unambiguously detect, quantify and enumerate spawning groups in available conventional data. This is because conventional data use line transects and other sparse sampling methods that have the potential to greatly undersample fish population distributions and groupings in space and time due to the vast regions that they inhabit and occupy (Godø et al., 2014; Johnsen, Rieucou, Ona, & Skaret, 2017; Letessier, Bouchet, & Meeuwig, 2017; Makris et al., 2006, 2009; National-Research-Council et al., 2015; Wang et al., 2016).

Both Atlantic cod and Atlantic herring are major oceanic fish species that are extremely important to ocean ecosystems. Atlantic cod is of the fish-feeding Gadidae family of top level predators. In contrast, Atlantic herring is of the plankton-feeding Clupeidae family of keystone species that are prey to many other fish, marine mammals and birds. Both families are found

1 INTRODUCTION	2
2 MATERIALS AND METHODS	2
3 RESULTS	3
4 DISCUSSION	6
5 CONCLUSIONS	10
ACKNOWLEDGEMENT	11
CONFLICT OF INTEREST	11
REFERENCES	11

throughout the world's oceans and are important in circulating biomass between open ocean and coastal waters via feeding to spawning cycles. Both families are extremely important economically and as a human food source (Duarte et al., 2009; FAO, 2013), as are many of the most abundant oceanic fish species. Atlantic cod and Atlantic herring in particular both have long economic and cultural histories in coastal North Atlantic and Arctic regions, where collapses and near collapses of their populations in Canada, the United States, the North Sea and Norway in the 20th to 21st centuries have led to economic turmoil for many coastal communities (Hilborn, Hively, Jensen, & Branch, 2014; Rose, 2007), and call for new survey methods with ecosystem-scale sensing (Jain, Ignisca, Yi, Ratilal, & Makris, 2013; US-Senate, 2011). Various other species of gadids such as walleye pollock, haddock, whiting and saithe, and clupeids such as sardines and sprats, also form large spawning groups that have traditionally been difficult or impossible to sense in their entirety.

2 | MATERIALS AND METHODS

We acquired instantaneous areal population density images of Atlantic cod spawning groups over wide areas in the Nordic Seas during February and March of 2014 with an OAWRS system configuration where the vertical source array and horizontal receiving array were towed from a single research vessel, RV Knorr. Wide area scattering strength images were produced by beamforming, matched filtering and charting the received OAWRS returns and then correcting for transmission loss (Andrews, Gong, & Ratilal, 2009; Gong et al., 2010; Jagannathan et al., 2009; Makris et al., 2006, 2009; Naftali & Makris, 2001). Linear frequency modulated (LFM) source waveform transmissions of 50 Hz bandwidth and 1-s duration centred at 955 Hz were used for the OAWRS cod measurements presented, which are above but within a decade of the expected swimbladder scattering resonance frequencies (Blaxter & Batty, 1990; Gong et al., 2010; Jagannathan et al., 2009; Jain et al., 2013; Love, 1978; Løvik & Hovem, 1979; Zhang, Liu, Ratilal, Cho, & Makris, 2017) of spawning cod in this region. Scattering strength was converted to areal population density by calibration with local

in situ measurements of areal population density obtained from vertical echo sounding. This calibration with conventional vertical echo sounding only affects the absolute level of the OAWRS population density estimate and not the relative levels or fish group morphology. The resulting population density estimates are consistent with those independently determined for the OAWRS measurements from scattering theory given measurements of local cod length and depth distributions (Appendix S1). The minimum cod population density detectable by OAWRS in the Nordic Seas was roughly 0.005 fish/m^2 (Makris et al., 2009), below which the data are contaminated by seafloor scattering mechanisms (Jagannathan, Küsel, Ratilal, & Makris, 2012; Jain et al., 2013; Makris & Ratilal, 2001). A five-octave horizontally towed line array towed at depths between 45 m and 60 m was used as the OAWRS receiver (Becker & Preston, 2003), where a mid-frequency aperture employing 64-hydrophones spaced at 0.75 m was used to collect the Nordic Seas cod data presented from transmissions sent by an 8-element vertical array with element spacing of 1 m towed at depths of 45 m to 60 m.

Raw OAWRS images are each comprised of hundreds of thousands of independent pixels since the OAWRS system has 15-m range resolution, and forms at least 64 independent horizontal beams, spanning ranges of many tens of kilometres. The angular resolution of any beam away from endfire varies as $\lambda/L \cos \theta$, where λ is the acoustic wavelength, L is the receiver array aperture length and θ is the horizontal angle from array broadside (Gong et al., 2010; Jagannathan et al., 2009; Makris et al., 2006). This angular resolution is enhanced by a statistically optimal deconvolution of the beamformed OAWRS data (Jain & Makris, 2016). To reduce the intensity standard deviation resulting from Gaussian field fluctuations (Makris, 1995, 1996) inherent in acoustic sensing of oceanic fish groups from waveguide transmission and scattering (Andrews, Gong, & Ratilal, 2011; Chen, Ratilal, & Makris, 2005; Ratilal & Makris, 2005), averaging of consecutive OAWRS images within a few minutes was employed, leading to a population density standard deviation of roughly 1 dB or 25% (Andrews, Chen, & Ratilal, 2009; Jagannathan et al., 2009; Makris et al., 2006; Tran, Andrews, & Ratilal, 2012). The instantaneous areal population density of Atlantic herring groups in the Gulf of Maine was acquired by a similar approach but in a bistatic framework where the OAWRS source and receiver were on separate research vessels as described in Makris et al. (2006) and Jagannathan et al. (2009).

To analyse Atlantic cod spawning group behaviour over long periods in the Nordic Seas, discrete spawning groups were detected and counted in 30 years of line-transect survey data collected from 1984 to 2014 in the primary Northeast Arctic spawning ground of Atlantic cod in Lofoten, Norway, using conventional downward directed acoustic echo sounding (Korsbrekke, 1997). This was done by spatially interpolating between line transects for each annual survey and segmenting regions at and above an empirically determined group boundary threshold density independently determined by a number of approaches using both line-transect and OAWRS measurements (Appendix S1).

The critical population density threshold characterizing the boundary of a cod shoal was consistently determined to be 0.016 fish/m^2 by a number of independent methods including: (a) least squares estimation with decades of line-transect survey data of cod in the Northeast Arctic spawning ground; (b) segmenting regions of high population density and gradient in OAWRS images; (c) segmenting regions of high population density and gradient in corresponding high-resolution line-transect vertical echosounder measurements; and (d) scaling the critical density consistently obtained experimentally with OAWRS for spawning group formation in another oceanic fish species (Makris et al., 2009) to account for functional dependencies on body length ratios (Appendix S1). This value of 0.016 fish/m^2 falls within the range found for cod group edge densities in Newfoundland of 0.007 to 0.020 fish/m^2 as measured by vertical acoustic echo sounding.

Cod spawning group size was then obtained by integrating the cod population density over each segmented region, where each year's spawning group size distribution integrated to the total ICES cod spawning population for that year (ICES, 2015). Regional group morphologies estimated from Northeast Arctic cod line-transect data in this manner were found to be consistent with those directly measured by instantaneous OAWRS imagery (Appendix S1). While historic line-transect data also exist for Atlantic herring in the Gulf of Maine, the line transects were spatially too sparse and temporally too intermittent to adequately sample herring spawning shoal morphology due to the temporally transient and spatially elongated nature of the herring groups (Makris et al., 2009, Appendix S2).

3 | RESULTS

We measured the instantaneous 2-D horizontal morphologies of entire vast Atlantic cod groups extending for tens of kilometres in length, covering thousands of square kilometres and containing millions of individuals, which to our knowledge have not been previously observed. These measurements were of the Northeast Arctic cod population in its primary spawning ground off the coast of Lofoten Norway, during the 2014 spawning period using OAWRS (Figure 1). The largest spawning group we observed spanned roughly 40 km in diameter, nearly $1/2$ degree in latitude, and was populated by at least 40 million cod (Figure 1b). It was found at the southern end of the Lofoten spawning ground where the densest concentrations surrounded the Island Røst. Here, the cod's preferred water depths of $100 \pm 20 \text{ m}$ (Appendix S1) approached rising seafloor about the island that curtailed further migrations inward. Such high cod concentrations surrounding Røst were observed to be spatially and temporally stable over days to weeks (Appendix S1) apparently in relation to the island's fixed bathymetric features. In contrast, at the northern end of the Lofoten spawning ground, near Andenes, smaller less dense groups of roughly 20 by 2 km and 1 million cod were observed (Figure 1c) to exhibit significant temporal and spatial variation over a period

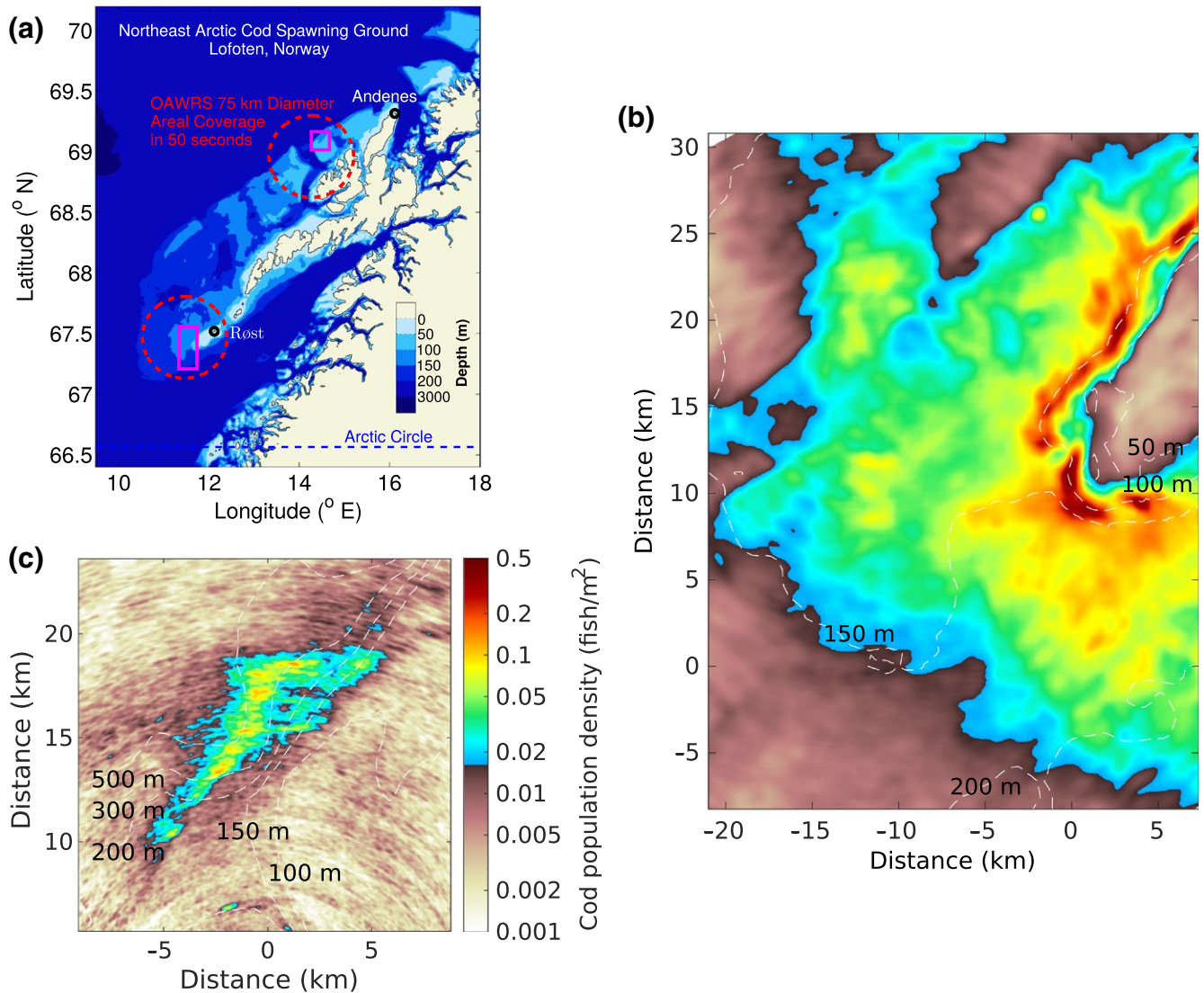


FIGURE 1 Spatial population distributions of entire Atlantic cod spawning groups of the Northeast Arctic obtained by instantaneous continental-shelf scale imaging. (a) Primary Northeast Arctic spawning ground of Atlantic cod (*Gadus morhua*), Lofoten, Norway. Red circles indicate OAWRS imaging coverage in 50 s. Regions where zoomed OAWRS cod population density image appear in (b) and (c) are indicated by purple rectangles. (b) Vast 40-km-diameter temporally stable cod group containing roughly 40 million individuals (152,000 tonnes) south of Røst Island comprising 17% of the estimated Lofoten cod spawning population. (c) Temporally transient lineated 20-km-scale cod group containing roughly 1 million individuals (3,800 tons) near Andenes, Norway. The colour scale transition from brown to blue occurs at the critical density of 0.016 fish/m² marking the cod group boundaries. Dashed white lines indicate water depth contours. Coordinate origins are at OAWRS Research Vessel Knorr locations: (b) 67.3°N, 11.5°E on February 23, 2014, 10:40:49 UTC; and (c) 69.0°N, 14.3°E on March 8, 2014, 00:16:49 UTC

of roughly 1–2 days and were not associated with specific bathymetric features.

We find that the mean group population per annual spawning season q_i of Northeast Arctic cod over the entire spawning ground in Lofoten Norway is relatively invariant across the available $M = 30$ years of line-transect survey data (Korsbrekke, 1997), averaging to $q = 1/M \sum_{i=1}^M q_i = 10.6$ million cod with a standard deviation of the annual mean $\left(\left[1/(M-1) \sum_{i=1}^M (q_i - q)^2 \right]^{1/2} \right)$ that is 36% of q , and no apparent temporal trend (Figures 2 and 3), where $q_i = 1/N_i \sum_{j=1}^{N_i} g_{ij}$ and g_{ij} denotes the j th cod spawning group size measured in the i th year. In contrast, larger variations in the

total annual spawning population with a standard deviation of 77% about the 125 million cod mean, including an increase of roughly 600% or more, were observed over this same 30-year period (Figure 4). This stability is also seen by the fact that since the mid-2000s, when the Northeast Arctic cod population returned to pre-industrial levels (Figure 4), the mean spawning group size of 11.1 million cod with a standard deviation of 25% has insignificant difference from that of the 30-year mean. The areal population density of cod groups was also found to be relatively stable with no apparent temporal trend and a standard deviation of 43% of the annual mean based solely on the 30-year line-transect vertical

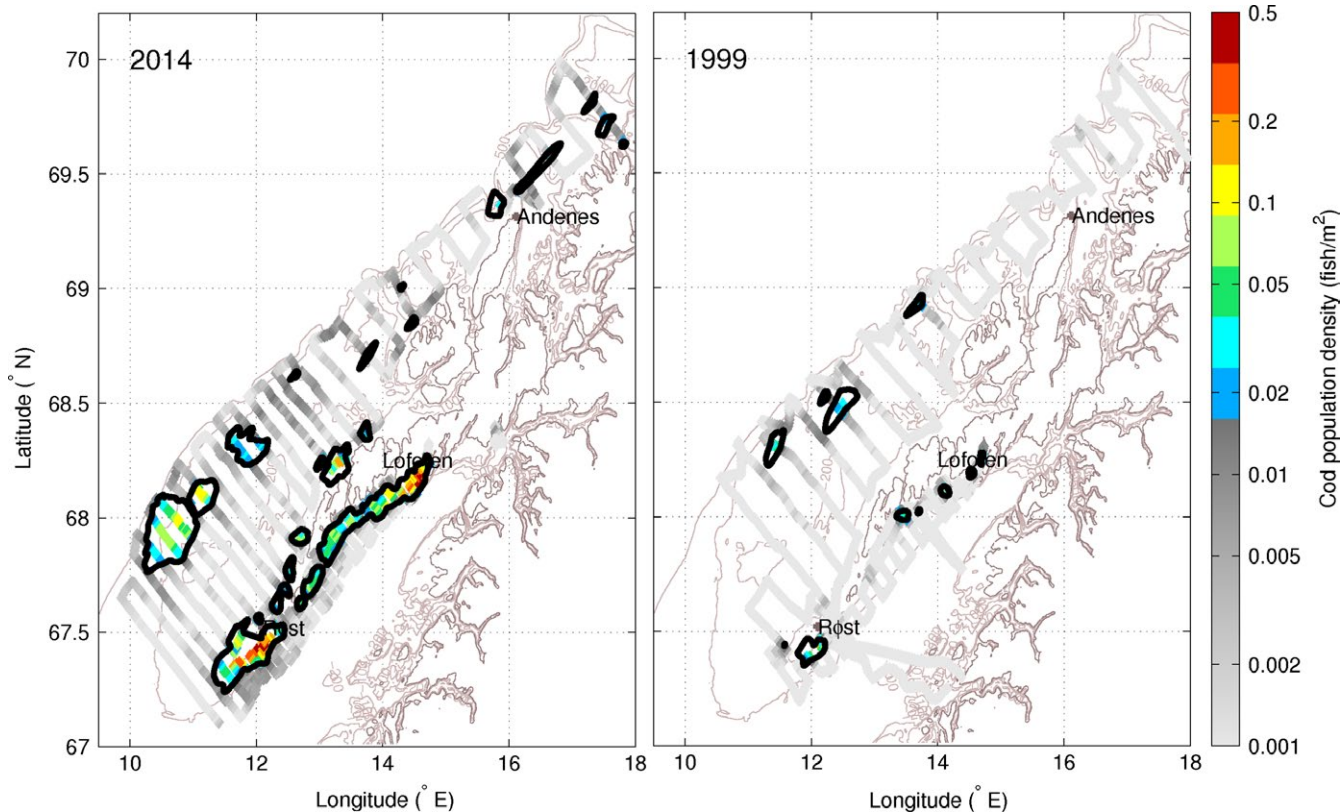


FIGURE 2 Atlantic cod population density along conventional line-transect surveys in the Northeast Arctic spawning ground of Lofoten Norway with downward directed echo sounding at 1-nmi resolution (Appendix S2). Discrete cod spawning groups are detected (black contours) and enumerated in three decades of line-transect survey data using group structural information obtained by OAWRS (Appendix S1). Example years of relatively high (2014) and relatively low (1999) cod abundance are shown

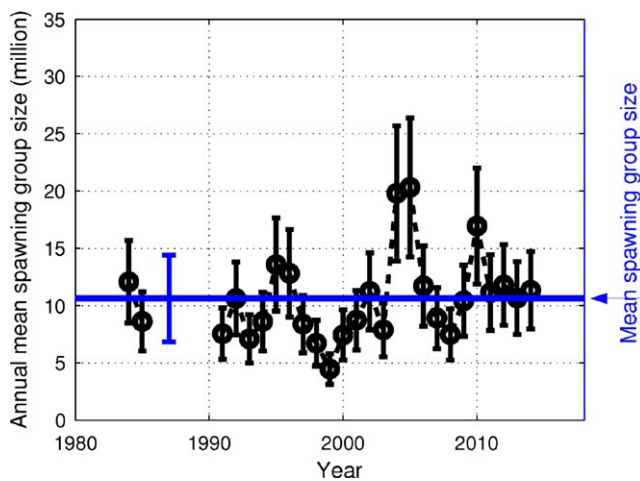


FIGURE 3 Mean annual spawning group population of Atlantic cod over the Northeast Arctic spawning ground of Lofoten Norway for 30 years of line-transect survey. Mean spawning group size over 30 years is 10.6 million (blue line) where the standard deviation of the annual mean is 36% (error bar)

echo sounding data. The annual mean areal density was found to range between 0.03 and 0.09 fish/m² based on a combination of the 30-year line-transect data and ICES spawning population estimates.

The size distribution of cod groups from 30 years of data in the Lofoten spawning ground is found to be consistent with a log-normal density (Figure 5a). The log-normal density is associated with growth processes that depend on many independent factors like those of the spawning cod groups in the Lofoten area (Blott & Pye, 2001; McCave, 1984; Wu, 1985). The log-normal density parametrically depends only on the mean and standard deviation of group size s . The standard deviation of group size over 30 years is found to be $\sigma = [1 / ((\sum_{i=1}^M N_i) - 1) \sum_{i=1}^M \sum_{j=1}^{N_i} (g_{ij} - q)^2]^{1/2} = 2q$, where q is the mean group size (10.6 million cod) over 30 years of data in the Lofoten spawning ground. The probability density governing annual spawning group size and the process leading to it can then be roughly characterized by

$$p_S(s) = \frac{1}{s\mu_2(q,\sigma)\sqrt{2\pi}} e^{-\frac{(\ln s - \mu_1(q,\sigma))^2}{2\mu_2^2(q,\sigma)}}, \quad (1)$$

where the mean of $\ln s$ is $\mu_1(q,\sigma) = \ln [q/\sqrt{1+(\sigma/q)^2}]$ and variance of $\ln s$ is $\mu_2^2(q,\sigma) = \ln [1+(\sigma/q)^2]$ as shown in Figure 5a. Time series of the annual spawning group size standard deviation $([1 / (N_i - 1) \sum_{j=1}^{N_i} (g_{ij} - q)^2]^{1/2})$ over 30 years is found to also have a mean of $2q$ and a standard deviation of 35%, indicating relative stability over the years (Figure 5b). Since the mid-2000s, when the Northeast Arctic cod population returned to pre-industrial levels, the standard deviation of spawning group size is within 35% of $\sigma = 2q$ and so has insignificant difference from that of the 30-year mean.

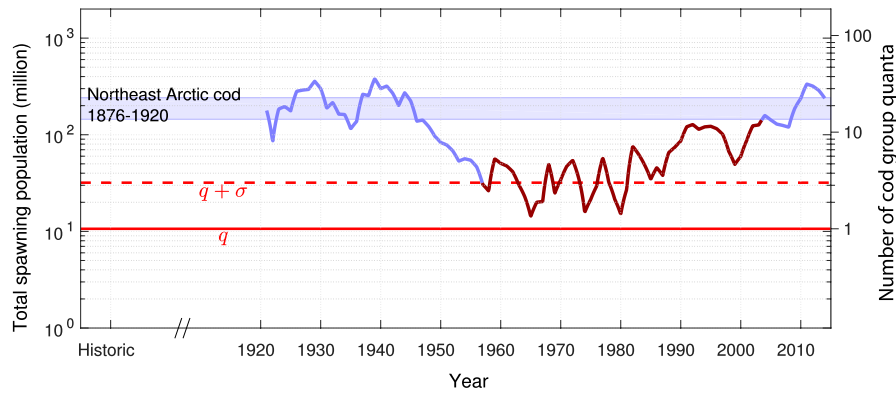


FIGURE 4 Time series of the total Atlantic cod spawning population of the Northeast Arctic Lofoten spawning ground. Large variations are seen over the last century. The time series is shown in brown from the time it declined to within a standard deviation of the cod group quantum ($q + \sigma$) to the time it returned to pre-industrial levels. The cod group quantum is the mean spawning group size (10.6 million) found for Atlantic cod in the Lofoten spawning ground from 1984 to 2014, which has insignificant difference from the mean when the population was at pre-industrial levels. The blue shaded area indicates the estimated spawning population level before the onset of industrial fishing in the early 20th century (Appendix S3)

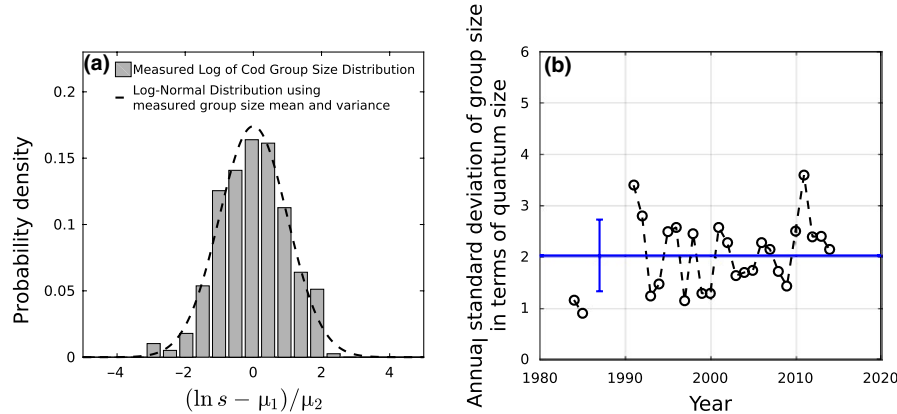


FIGURE 5 (a) Histogram of cod spawning group size in the Northeast Arctic spawning ground of Lofoten Norway over 30 years from 1984 to 2014 after log transformation. The abscissa is $(\ln s - \mu_1) / \mu_2$ where s is measured cod group size, q is the measured mean (10.6 million cod) and $\sigma = 2q$ is the measured standard deviation of s over the 30-year data set, $\mu_1(q, \sigma) = \ln [q / \sqrt{1 + (\sigma/q)^2}]$ and $\mu_2^2(q, \sigma) = \ln [1 + (\sigma/q)^2]$. The histogram of the natural logarithm of the cod spawning group size obtained from the 30-year line-transect echosounder data is consistent with a Gaussian probability density distribution (dashed curve) for $\ln s$ and a log-normal distribution for s (Eq. 1) using the measured values for the mean q and standard deviation σ of s . (b) Time series of the annual standard deviation of spawning group size measured in units of mean group size q or quantum size. The mean of this time series is approximately $2q$, and the standard deviation is 35% of this mean

4 | DISCUSSION

Pre-industrial hindcasts for the 19th century combined with available data over roughly the last century indicate that the total Northeast Arctic cod spawning population has not fallen below the mean spawning group size measured here in these time periods (Figure 4). It is noteworthy that the mean spawning group size over the entire 30-year period of available data has negligible difference from that over years when the total population was at pre-industrial levels. The total population did decline to within a standard deviation σ of the mean spawning group size q at pre-industrial levels and then took decades to return to pre-industrial levels. This is apparently a consequence of the large difference between the total pre-industrial spawning population and the standard deviation augmented mean

spawning group quantum found at pre-industrial levels, which is many times smaller.

Group behaviour during spawning is also investigated for the Atlantic herring species, which are total breeders, releasing one batch of eggs per season, as opposed to cod which are batch spawners, whose individuals each strive to release multiple batches following multiple courtships across an entire annual spawning season. These two species then have fundamental differences in their spawning strategies that are representative of spawning found in oceanic fish. In the fall of 2006, large Atlantic herring groups (Figure 6a) were observed to follow a consistent daily process over the peak Georges Bank spawning period whereby a group would form on the northern flank of the Georges Bank near sunset and migrate to shallower regions on the bank to spawn under cover of darkness (Makris et al.,

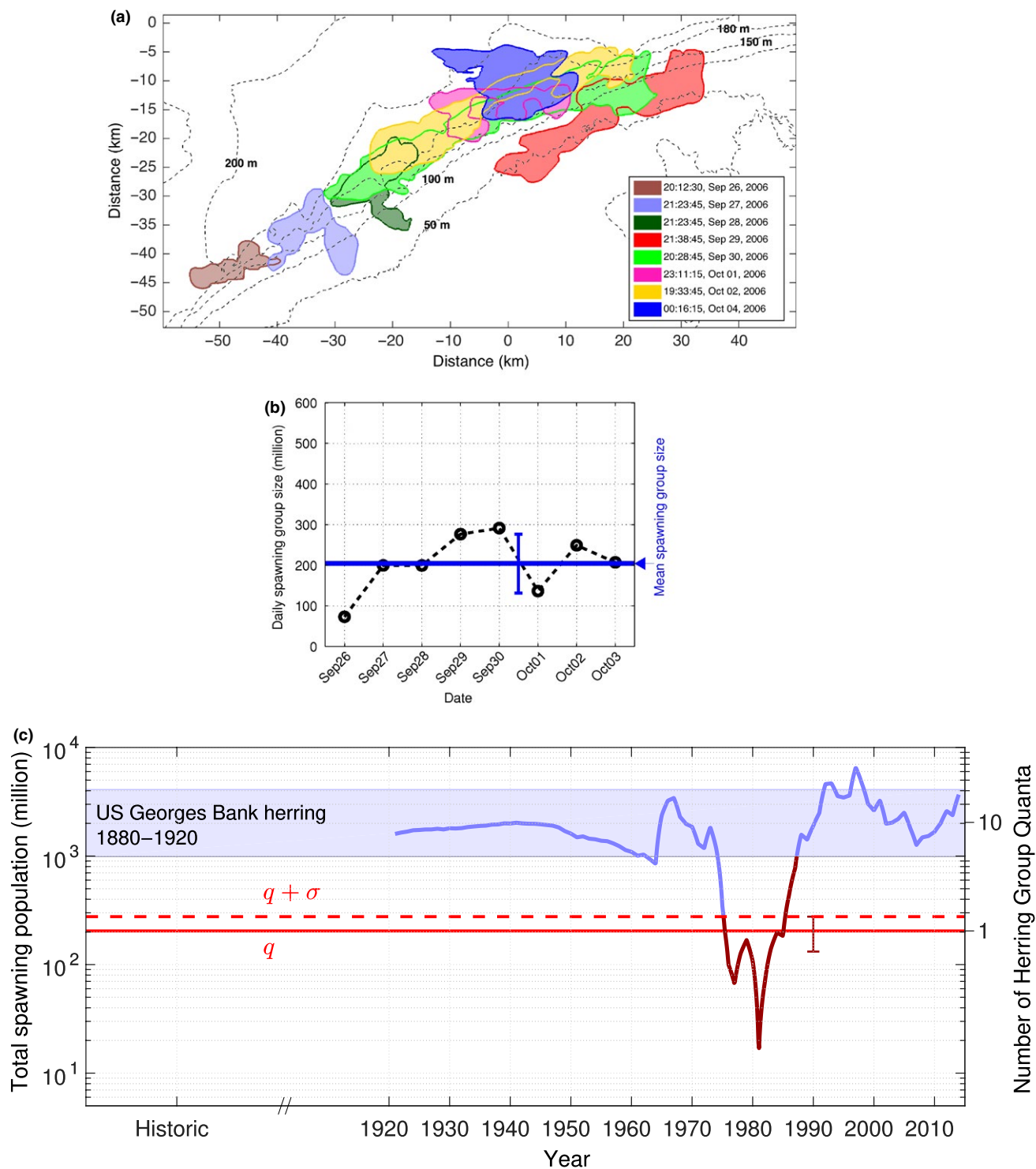


FIGURE 6 Mean spawning group size and total spawning population of Atlantic herring in Georges Bank. (a) Location of the daily spawning herring group on the northern flank of Georges bank during the 8-day peak spawning period in the Fall of 2006 determined by OAWRS imagery. Group boundaries occur at the group formation critical density of 0.2 fish/m² for herring (Makris et al., 2009). (b) Daily spawning group population over the peak spawning period obtained from instantaneous OAWRS images of each group. Spawning group population has a mean of 204 million (blue line) and a standard deviation of 35% (error bar) over the peak spawning period in 2006. (c) Time series of the total Atlantic herring spawning population in the Georges Bank spawning ground. Large variations are seen over the last century. The time series is shown in brown from the time it declined to within a standard deviation of the herring group quantum to the time it returned to pre-industrial levels. The herring group quantum is the mean spawning group size (204 million) found for Atlantic herring, which was found when the total population was at pre-industrial levels. The blue shaded area indicates the estimated spawning population level before the onset of industrial fishing in the early 20th century (Appendix S3). The OAWRS sensor location on 4 October 2006, 00:16:15 EDT, at 42.2°N, 67.7°W is the coordinate origin in (a)

2009). If each herring goes through the spawning grouping process only once, as has been previously established (Brander, 2005), the sum of the daily group populations over the spawning period should equal the total Georges Bank spawning population. This is indeed demonstrated by consistency to within 7% of the NOAA Fisheries estimate of the total Georges Bank spawning population of 1.74 billion for 2006 which required weeks to months of conventional sampling (NEFSC, 2012) and the 1.63 billion estimate independently obtained by summing the daily spawning group populations over the peak spawning period from a single instantaneous OAWRS image each day (Figure 6b).

We find the daily spawning group population of 204 million Atlantic herring on average to be relatively stable with a standard deviation of 35% of the mean over the peak spawning period (Figure 6b). The 2006 measurements were made in a period when the total spawning population was at or above estimated pre-industrial levels (Figure 6c). Pre-industrial hindcasts for the 19th century (Appendix S3) combined with available data over roughly the last century indicate that the total spawning population of Georges Bank herring in the mid-1970s fell below the mean plus standard deviation ($q + \sigma$)

spawning group level that was measured when the total spawning population was at or above pre-industrial levels in 2006. It then took over a decade for the total population to return to pre-industrial levels (Figure 6c), apparently due to the large difference between the pre-industrial total level and that of the mean group size measured when the population was at pre-industrial levels.

Coincidence between the inability to detect large spawning groups with conventional survey methods and fish population depletion has been noted (Cardinale & Svedäng, 2004; Rose & Rowe, 2015; Vitale, Borjesson, Svedäng, & Casini, 2008). In this context, no other quantification of the statistical distribution or statistical moments of the size of Atlantic cod spawning groups than that provided here for the Nordic Seas is available for populations at or near pre-industrial levels, to our knowledge. As a point of discussion, spawning group sizes found here within a standard deviation of the mean ($q \pm \sigma$) for the Northeast Arctic population of Atlantic cod cover a large range that is not inconsistent with evidence found in other regions of the North Atlantic obtained from line-transect surveys (e.g., Gurshin, Howell, & Jech, 2013; Jain et al., 2013; Rose, 1993, 2007; Rose & Rowe, 2015). It has been noted

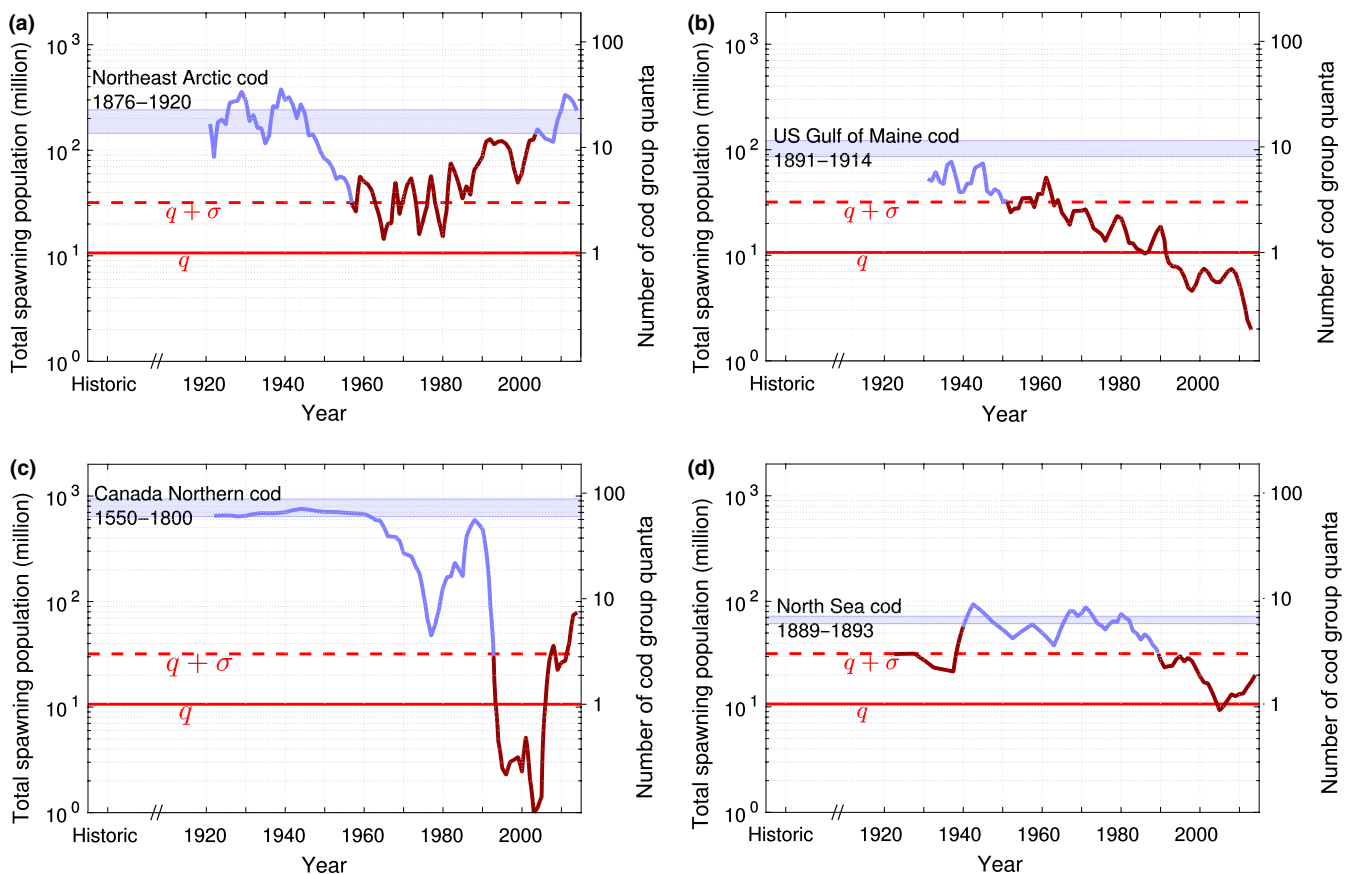


FIGURE 7 Time series of total Atlantic cod spawning populations at major spawning grounds in the North Atlantic show large variations over the last century. Time series for a total spawning population are shown in brown from the time they decline to within a standard deviation of the cod group quantum found for the Northeast Arctic population (only available data) to the time they return to pre-industrial levels. The cod group quantum is the mean spawning group size (10.6 million) found for Atlantic cod in the Lofoten spawning ground from 1984–2014, which has insignificant difference from the mean when the population was at pre-industrial levels. The blue shaded areas indicate the estimated spawning population levels in indicated regions before the onset of industrial fishing in the early 20th century (Appendix S3)

that q and σ over 30 years of Northeast Arctic data have insignificant difference from the values found when the population was at pre-industrial levels. These Northeast Arctic statistics are then used as the only available empirical metrics for the nominal range of cod spawning group sizes at pre-industrial levels when examining spawning population time series at other locations in the North Atlantic, where relevant environmental conditions are reasonably similar (McBride et al., 2015). Time series of the total Atlantic cod spawning population for major spawning regions across the North Atlantic (Figure 7) show that once the total spawning population declined to within a standard deviation of the mean cod spawning group size quantum derived for the Northeast Arctic population at pre-industrial levels, return of the total spawning population to pre-industrial levels did not occur in that region even after decades, as quantified in more detail in Appendix S3. This is apparently a consequence of the large difference between any total pre-industrial spawning population and the standard deviation augmented mean of spawning group size found in the Northeast Arctic. The cod population time series in these various

regions do not consistently show higher variance in growth rate for smaller populations (Appendix S3). As with Atlantic cod, to our knowledge, no other quantification of the mean size of Atlantic herring spawning groups is available for populations at or near pre-industrial levels. To continue the discussion, the mean spawning group size measured for Georges Bank herring here is then used as the only available metric for the nominal mean spawning group size of herring at pre-industrial levels when examining spawning population time series at other locations in the North Atlantic. Time series of the Atlantic herring spawning population for major spawning grounds across the North Atlantic (Figure 8) show that when total spawning population declined to within a standard deviation of the mean spawning group size measured for Georges Bank herring at pre-industrial levels in 2006, return of the total spawning population to pre-industrial levels required decades, as quantified in more detail in Appendix S3. Again, this is apparently a consequence of the large difference between the total pre-industrial spawning population and the mean Georges Bank spawning group size.

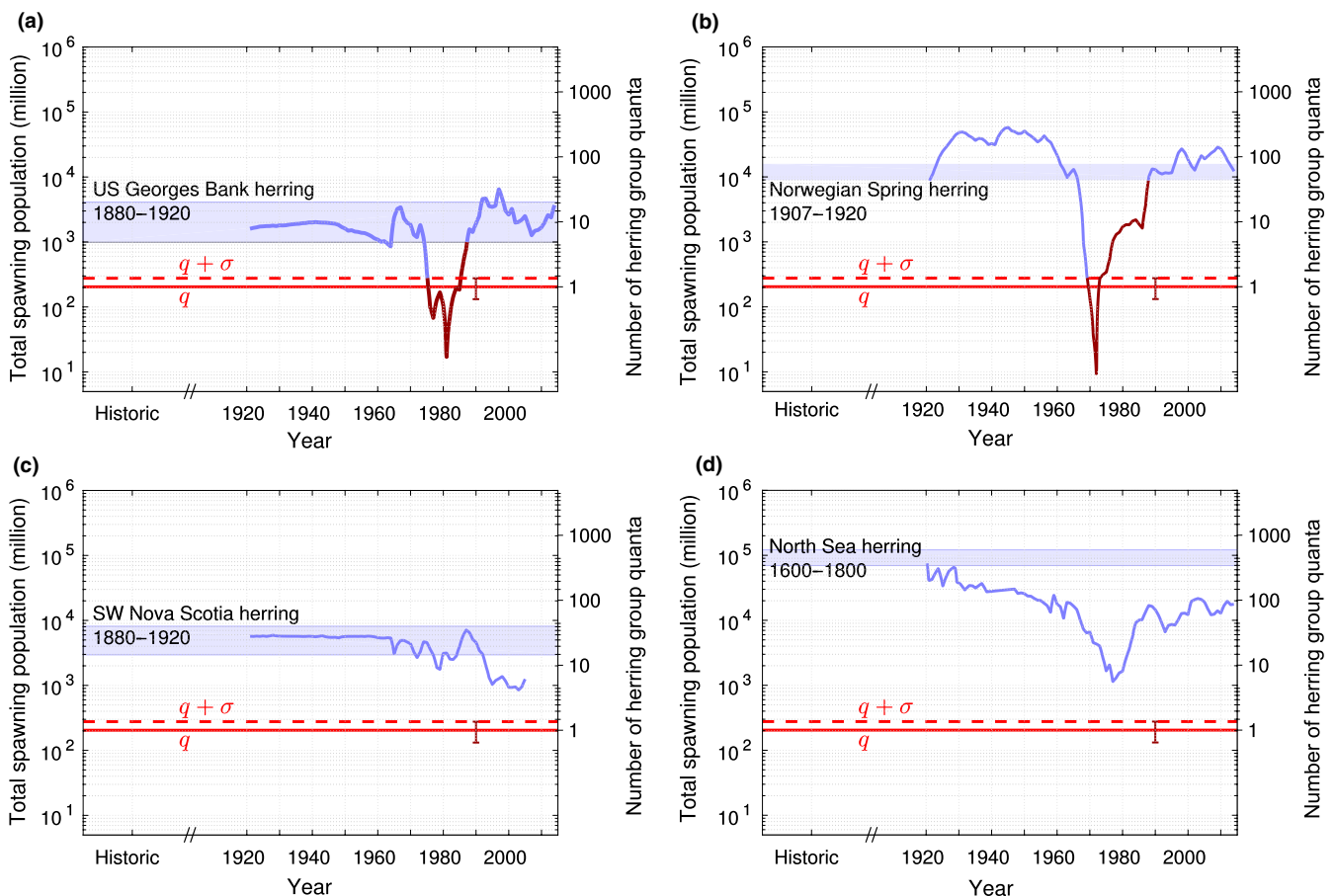


FIGURE 8 Total spawning population time series of herring at major spawning grounds across the North Atlantic. The total spawning populations show large variations over the last century at these major spawning grounds in the North Atlantic. Time series for a total spawning population are shown in brown from the time they decline to within a standard deviation of the herring group quantum found for the Georges Bank population (only available data) to the time they return to pre-industrial levels. The herring group quantum for Georges Bank is the mean spawning group size (204 million) found for Atlantic herring in Georges Bank when the total population was at pre-industrial levels. The blue shaded areas are the estimated spawning population levels in indicated regions before the onset of industrial fishing in the early 20th century (Appendix S3)

We are unaware of any previous multi-decadal quantification of the empirical size distribution of the behavioural groups found at spawning for any oceanic fish species. Given this, the presented comparisons between the relative size of total spawning populations over time and the mean spawning group size at pre-industrial levels are intended to provide potentially useful insights regarding the relationships between scales of natural group behavioural processes within a population and those of the overall population.

Regardless of the mechanisms that lead to the distribution of a spawning population into many distributed groups, which are not completely understood, such diversification may increase the probability of robust reproduction by enabling greater advantage to be taken of spatial and temporal variations or fluctuations in the environment. During feeding, cod in particular behave as individual predators (Godø & Michalsen, 2000; Rose, 1993). During spawning, a significant amount of energy is invested in group behavioural processes where known advantages include a highly increased mate-encounter rate which leads to improved mate choice and increased egg fertilization rates as well as time-space alignment to enable synchronized batch spawning (Krause & Ruxton, 2002; Makris et al., 2009; Molloy, Côte, & Reynolds, 2012). Too large a spawning group, however, may potentially result in disadvantages including extra energy costs to maintain the group, nutrient depletion, environmental pollution, expansion into unfavourable environments and increased risk contamination from diseases and parasites (Krause & Ruxton, 2002; Molloy et al., 2012).

Spawning group size apparently grows in accord with many independent influencing factors, as exhibited by the log-normal size distribution for cod spawning groups found here, and may have invariant properties if the entire stochastic system of influencing factors and responses can attain stable equilibria. An example would be a nonlinear physical system that only behaves asymptotically as a stable linear harmonic oscillator near equilibrium for a certain range of parameters (Strogatz, 2014). This classic concept in physical systems could potentially apply to and explain the relative stability of the mean spawning group size found in the present study for each species and population investigated. Similar processes may be at work with other oceanic fish that form large groups, where group sizes may exhibit relatively invariant means or quantum-like properties on average under certain conditions. A number of recent studies have shown results not inconsistent with this quantum concept of a stable equilibrium possible for mean group size and higher statistical moments (Brierley & Cox, 2015; Jech & Stroman, 2012; Reuchlin-Hugenholtz, Shackell, & Hutchings, 2015, 2016). In this conceptual framework, since natural selection is on the individual, evolutionary pressures favour individuals that develop traits aligned with stable and reliable means of survival.

5 | CONCLUSIONS

We have investigated the wide-area group behavior of spawning Atlantic cod by obtaining first-look images of the instantaneous population density of entire cod spawning groups stretching for tens of kilometres in the Nordic Seas by a combination of Ocean

Acoustic Waveguide Remote Sensing (OAWRS) and conventional acoustic methods. With the structural information obtained in this manner about entire spawning groups and their boundaries, it was possible to quantify the spawning group size distribution of cod over a roughly 30 year period from line-transect data collected in the Nordic seas via conventional vertical echo sounding. This size distribution is found to be consistent with the log-normal probability density, which is often found in growth processes that depend on many independent factors, as is the case for Atlantic cod groups in the Nordic Seas. Total annual spawning populations of cod in the Nordic Seas are found to distribute into many vast behavioural groups during spawning with relatively stable mean size despite larger variations in total spawning population over the decades of available data. It may eventually be possible to quantitatively model the processes leading to these groups sizes through a nonlinear stochastic system approach where stable mean group sizes over years may be related to locations of stable equilibrium. Comparisons were made of the total spawning population over roughly the last century in the Nordic Seas with spawning group size statistics obtained here, which provide a scale of internal group behavioural structure within the population. When sustained at pre-industrial levels, the total spawning population was found to greatly exceed the mean spawning group size. As an apparent consequence of this large differential, when the total population came to within a standard deviation of this mean cod spawning group quantum, that is when the overall scale of the population converged with the inner-group behavioural scale we found, return to pre-industrial levels required decades. This is consistent with reported coincidences between the inability to detect large cod spawning groups with conventional survey methods and fish population depletion (Cardinale & Svedäng, 2004; Rose & Rowe, 2015; Vitale et al., 2008). Similar results are found for Atlantic herring, another species of oceanic fish that follow a significantly different spawning strategy, suggesting that analysis of other oceanic fish that form vast spawning groups may lead to corresponding findings. This is significant because many of the abundant oceanic fish species that form vast spawning groups are of critical importance to ocean ecosystems. Finally, it is noteworthy that summing the spawning group population found in a single instantaneous OAWRS image per day over the 8-day peak spawning period, with less than one hour of conventional acoustics for calibration, enabled accurate enumeration of the entire Georges Bank herring spawning population to within 7% of the independent NOAA Fisheries estimate for 2006, which required weeks to months of conventional sampling, suggesting that such an approach may have future potential for population assessment.

ACKNOWLEDGEMENT

This work was sponsored by the Norwegian Institute of Marine Research (IMR), the Office of Naval Research (ONR) and the National Science Foundation (NSF). We thank the captains, officers and crews of the research vessels Knorr, Johan Hjort and the fishing vessel Artus. We thank our engineers at sea: John Preston,

Marcus Hursh, Michael Einhorn, Chad Smith, Scott Whitney, Carl Stevens, Jim Dorminy, Paul Zimpelman and William Ang. We thank Knut Korsbrekke of IMR for helpful discussions. We thank the National Oceanic and Atmospheric Administration (NOAA) and the Norwegian Defense Research Establishment (FFI) for additional support.

CONFLICT OF INTEREST

The authors declare no conflict of interest.

ORCID

Nicholas C. Makris  <http://orcid.org/0000-0003-4369-296X>

Olav Rune Godø  <https://orcid.org/0000-0001-8826-8068>

Gavin J. Macaulay  <http://orcid.org/0000-0003-2518-6537>

Byunggu Cho  <http://orcid.org/0000-0003-4926-2792>

Josef Michael Jech  <https://orcid.org/0000-0002-7691-6643>

REFERENCES

- Andrews, M., Chen, T., & Ratilal, P. (2009). Empirical dependence of acoustic transmission scintillation statistics on bandwidth, frequency, and range in New Jersey continental shelf. *The Journal of the Acoustical Society of America*, 125(1), 111–124. <https://doi.org/10.1121/1.3037228>
- Andrews, M., Gong, Z., & Ratilal, P. (2009). High resolution population density imaging of random scatterers with the matched filtered scattered field variance. *The Journal of the Acoustical Society of America*, 126(3), 1057–1068. <https://doi.org/10.1121/1.3177271>
- Andrews, M., Gong, Z., & Ratilal, P. (2011). Effects of multiple scattering, attenuation and dispersion in waveguide sensing of fish. *The Journal of the Acoustical Society of America*, 130(3), 1253–1271. <https://doi.org/10.1121/1.3614542>
- Becker, K., & Preston, J. (2003). The onr five octave research array (fora) at Penn state. In *Oceans 2003. Proceedings* (Vol. 5, pp. 2607–2610). IEEE.
- Berdahl, A., Westley, P. A., Levin, S. A., Couzin, I. D., & Quinn, T. P. (2016). A collective navigation hypothesis for homeward migration in anadromous salmonids. *Fish and Fisheries*, 17(2), 525–542. <https://doi.org/10.1111/faf.12084>
- Blaxter, J., & Batty, R. (1990). "Swimbladder behaviour" and target strength. *Rapports et Proces-verbaux des Réunions du Conseil International pour l'Exploration de la Mer*, 189, 233–244.
- Blott, S. J., & Pye, K. (2001). Gradistat: A grain size distribution and statistics package for the analysis of unconsolidated sediments. *Earth Surface Processes and Landforms*, 26(11), 1237–1248. <https://doi.org/10.1002/esp.261>
- Brander, K. (2005). *Spawning and life history information for north Atlantic cod stocks*. ICES cooperative research report.
- Brierley, A. S., & Cox, M. J. (2015). Fewer but not smaller schools in declining fish and krill populations. *Current Biology*, 25(1), 75–79. <https://doi.org/10.1016/j.cub.2014.10.062>
- Cardinale, M., & Svedäng, H. (2004). Modelling recruitment and abundance of Atlantic cod, *Gadus morhua*, in the eastern Skagerrak-Kattegat (north sea): Evidence of severe depletion due to a prolonged period of high fishing pressure. *Fisheries Research*, 69(2), 263–282. <https://doi.org/10.1016/j.fishres.2004.04.001>
- Chen, T., Ratilal, P., & Makris, N. C. (2005). Mean and variance of the forward field propagated through three-dimensional random internal waves in a continental-shelf waveguide. *The Journal of the Acoustical Society of America*, 118(6), 3560–3574. <https://doi.org/10.1121/1.1993107>
- Croft, D. P., Krause, J., Couzin, I. D., & Pitcher, T. J. (2003). When fish shoals meet: Outcomes for evolution and fisheries. *Fish and Fisheries*, 4(2), 138–146. <https://doi.org/10.1046/j.1467-2979.2003.00113.x>
- Duarte, C. M., Holmer, M., Olsen, Y., Soto, D., Marbà, N., Guiu, J., ... Karakassis, I. (2009). Will the oceans help feed humanity? *BioScience*, 59(11), 967–976. <https://doi.org/10.1525/bio.2009.59.11.8>
- FAO. (2013). *Fao yearbook of fishery statistics summary tables*. Retrieved from <ftp://ftp.fao.org/FI/STAT/summary/a1d.pdf>.
- Godø, O. R., Handegard, N. O., Browman, H. I., Macaulay, G. J., Kaartvedt, S., Giske, J., ... Johnsen, E. (2014). Marine ecosystem acoustics (mea): Quantifying processes in the sea at the spatio-temporal scales on which they occur. *ICES Journal of Marine Science*, 71(8), 2357–2369. <https://doi.org/10.1093/icesjms/fsu116>
- Godø, O. R., & Michalsen, K. (2000). Migratory behaviour of north-east arctic cod, studied by use of data storage tags. *Fisheries Research*, 48(2), 127–140. [https://doi.org/10.1016/S0165-7836\(00\)00177-6](https://doi.org/10.1016/S0165-7836(00)00177-6)
- Gong, Z., Andrews, M., Jagannathan, S., Patel, R., Jech, J. M., Makris, N. C., & Ratilal, P. (2010). Low-frequency target strength and abundance of shoaling Atlantic herring (*Clupea harengus*) in the gulf of Maine during the ocean acoustic waveguide remote sensing 2006 experiment. *The Journal of the Acoustical Society of America*, 127(1), 104–123. <https://doi.org/10.1121/1.3268595>
- Gurshin, C. W., Howell, W. H., & Jech, J. M. (2013). Synoptic acoustic and trawl surveys of spring-spawning Atlantic cod in the gulf of Maine cod spawning protection area. *Fisheries Research*, 141, 44–61. <https://doi.org/10.1016/j.fishres.2012.09.018>
- Hilborn, R., Hively, D. J., Jensen, O. P., & Branch, T. A. (2014). The dynamics of fish populations at low abundance and prospects for rebuilding and recovery. *ICES Journal of Marine Science*, 71(8), 2141–2151. <https://doi.org/10.1093/icesjms/fsu035>
- ICES. (2015). *Ices 2015 afwg report*. Retrieved from <http://www.ices.dk/sites/pub/Publication%20Reports/Expert%20Group%20Report/acom/2015/AFWG/01%20AFWG%20Report%202015.pdf>.
- Jagannathan, S., Bertsatos, I., Symonds, D., Chen, T., Nia, H. T., Jain, A. D., ... Makri, N. C. (2009). Ocean acoustic waveguide remote sensing (OAWRS) of marine ecosystems. *Marine Ecology Progress Series*, 395, 137–160. <https://doi.org/10.3354/meps08266>
- Jagannathan, S., Küsel, E. T., Ratilal, P., & Makris, N. C. (2012). Scattering from extended targets in range-dependent fluctuating ocean-waveguides with clutter from theory and experiments. *The Journal of the Acoustical Society of America*, 132(2), 680–693. <https://doi.org/10.1121/1.4726073>
- Jain, A. D., Ignisca, A., Yi, D. H., Ratilal, P., & Makris, N. C. (2013). Feasibility of ocean acoustic waveguide remote sensing (OAWRS) of Atlantic cod with seaoor scattering limitations. *Remote Sensing*, 6(1), 180–208. <https://doi.org/10.3390/rs6010180>
- Jain, A. D., & Makris, N. C. (2016). Maximum likelihood deconvolution of beamformed images with signal-dependent speckle fluctuations from Gaussian random fields: With application to ocean acoustic waveguide remote sensing (OAWRS). *Remote Sensing*, 8(9), 694. <https://doi.org/10.3390/rs8090694>
- Jech, J. M., & Stroman, F. (2012). Aggregative patterns of pre-spawning Atlantic herring on Georges bank from 1999–2010. *Aquatic Living Resources*, 25(1), 1–14. <https://doi.org/10.1051/alr/2012003>
- Johnsen, E., Rieucan, G., Ona, E., & Skaret, G. (2017). Collective structures anchor massive schools of lesser Sandeel to the seabed, increasing vulnerability to fishery. *Marine Ecology Progress Series*, 573, 229–236. <https://doi.org/10.3354/meps12156>

- Klemas, V. (2013). Fisheries applications of remote sensing: An overview. *Fisheries Research*, 148, 124–136. <https://doi.org/10.1016/j.fishres.2012.02.027>
- Korsbrekke, K. (1997). *Norwegian acoustic survey of north east arctic cod on the spawning grounds off lofoten*. Report No. ICES Document CM 1997/Y:18.
- Koslow, J. A. (2009). The role of acoustics in ecosystem-based fishery management. *ICES Journal of Marine Science*, 66(6), 966–973. <https://doi.org/10.1093/icesjms/fsp082>
- Krause, J., & Ruxton, G. D. (2002). *Living in groups*. Oxford, UK: Oxford University Press.
- Letessier, T. B., Bouchet, P. J., & Meeuwig, J. J. (2017). Sampling mobile oceanic fishes and sharks: Implications for fisheries and conservation planning. *Biological Reviews*, 92(2), 627–646. <https://doi.org/10.1111/brv.12246>
- Love, R. H. (1978). Resonant acoustic scattering by swimbladder-bearing fish. *The Journal of the Acoustical Society of America*, 64(2), 571–580. <https://doi.org/10.1121/1.382009>
- Løvik, A., & Hovem, J. M. (1979). An experimental investigation of swimbladder resonance in fishes. *The Journal of the Acoustical Society of America*, 66(3), 850–854. <https://doi.org/10.1121/1.383238>
- Mackinson, S., Sumaila, U. R., & Pitcher, T. J. (1997). Bioeconomics and catchability: Fish and fishers behaviour during stock collapse. *Fisheries Research*, 31(1–2), 11–17. [https://doi.org/10.1016/S0165-7836\(97\)00020-9](https://doi.org/10.1016/S0165-7836(97)00020-9)
- Makris, N. C. (1995). A foundation for logarithmic measures of fluctuating intensity in pattern recognition. *Optics Letters*, 20(19), 2012–2014. <https://doi.org/10.1364/OL.20.002012>
- Makris, N. C. (1996). The effect of saturated transmission scintillation on ocean acoustic intensity measurements. *The Journal of the Acoustical Society of America*, 100(2), 769–783. <https://doi.org/10.1121/1.416239>
- Makris, N. C., & Ratilal, P. (2001). A unified model for reverberation and submerged object scattering in a stratified ocean waveguide. *The Journal of the Acoustical Society of America*, 109(3), 909–941. <https://doi.org/10.1121/1.1339826>
- Makris, N. C., Ratilal, P., Jagannathan, S., Gong, Z., Andrews, M., Bertsatos, I., ... Jech, J. M. (2009). Critical population density triggers rapid formation of vast oceanic fish shoals (with supporting online material). *Science*, 323(5922), 1734–1737. <https://doi.org/10.1126/science.1169441>
- Makris, N. C., Ratilal, P., Symonds, D. T., Jagannathan, S., Lee, S., & Nero, R. W. (2006). Fish population and behavior revealed by instantaneous continental shelf-scale imaging (with supporting online material). *Science*, 311(5761), 660–663. <https://doi.org/10.1126/science.1121756>
- McBride, R. S., Somarakis, S., Fitzhugh, G. R., Albert, A., Yarangina, N. A., Wuenschel, M. J., ... Basilone, G. (2015). Energy acquisition and allocation to egg production in relation to fish reproductive strategies. *Fish and Fisheries*, 16(1), 23–57. <https://doi.org/10.1111/faf.12043>
- McCave, I. (1984). Size spectra and aggregation of suspended particles in the deep ocean. *Deep Sea Research Part A. Oceanographic Research Papers*, 31(4), 329–352. [https://doi.org/10.1016/0198-0149\(84\)90088-8](https://doi.org/10.1016/0198-0149(84)90088-8)
- Molloy, P. P., Côte, I. M., & Reynolds, J. D. (2012). Why spawn in aggregations? In S. de Mitcheson, Y. Colin, & L. Patrick (Eds.), *Reef fish spawning aggregations: Biology, research and management* (pp. 57–83). New York, NY: Springer. <https://doi.org/10.1007/978-94-007-1980-4>
- Naftali, E., & Makris, N. C. (2001). Necessary conditions for a maximum likelihood estimate to become asymptotically unbiased and attain the Cramer-Rao lower bound. Part I. General approach with an application to time-delay and Doppler shift estimation. *The Journal of the Acoustical Society of America*, 110(4), 1917–1930. <https://doi.org/10.1121/1.1387091>
- National-Research-Council, Division on Engineering and Physical Sciences, Board on Mathematical Sciences and Their Applications, Committee on Applied and Theoretical Statistics (2015). *Robust methods for the analysis of images and videos for fisheries stock assessment: Summary of a workshop*. Washington, DC: National Academies Press.
- NEFSC. (2012). *54th northeast regional stock assessment workshop (54th saw) assessment re-port*. Retrieved from <http://www.nefsc.noaa.gov/publications/crd/crd1218/>. NOAA National Marine Fisheries Service, Northeast Fisheries Science Center, 166 Water Street, Woods Hole, MA 02543.
- Nicol, S., & Brierley, A. S. (2010). Through a glass less darkly new approaches for studying the distribution, abundance and biology of euphausiids. *Deep Sea Research Part II: Topical Studies in Oceanography*, 57(7–8), 496–507. <https://doi.org/10.1016/j.dsr2.2009.10.002>
- Pitcher, T. J. (1986). Functions of shoaling behaviour in teleosts. In T. J. Pitcher (Ed.), *The behaviour of teleost fishes* (pp. 294–337). Berlin, Germany: Springer. <https://doi.org/10.1007/978-1-4684-8261-4>
- Pitcher, T. J., Hart, P., & Pauly, D. (2012). *Reinventing fisheries management*, Vol. 23. Berlin, Germany: Springer Science & Business Media.
- Ratilal, P., & Makris, N. C. (2005). Mean and covariance of the forward field propagated through a stratified ocean waveguide with three-dimensional random inhomogeneities. *The Journal of the Acoustical Society of America*, 118(6), 3532–3559. <https://doi.org/10.1121/1.1993087>
- Reuchlin-Hugenholtz, E., Shackell, N. L., & Hutchings, J. A. (2015). The potential for spatial distribution indices to signal thresholds in marine fish biomass. *PLoS ONE*, 10(3), e0120500. <https://doi.org/10.1371/journal.pone.0120500>
- Reuchlin-Hugenholtz, E., Shackell, N. L., & Hutchings, J. A. (2016). Spatial reference points for groundfish. *ICES Journal of Marine Science*, 73(10), 2468–2478. <https://doi.org/10.1093/icesjms/fsw123>
- Ritz, D. A., Hobday, A. J., Montgomery, J. C., & Ward, A. J. (2011). Social aggregation in the pelagic zone with special reference to fish and invertebrates. In D. W. Sims (Ed.), *Advances in marine biology*, Vol. 60 (pp. 161–227). Amsterdam, The Netherlands: Elsevier.
- Rose, G. A. (1993). Cod spawning on a migration highway in the north-west Atlantic. *Nature*, 366(6454), 458. <https://doi.org/10.1038/366458a0>
- Rose, G. A. (2007). *Cod: The ecological history of the north Atlantic fisheries*. St. John's, NL: Breakwater Books.
- Rose, G. A., & Rowe, S. (2015). Northern cod comeback. *Canadian Journal of Fisheries and Aquatic Sciences*, 72(12), 1789–1798. <https://doi.org/10.1139/cjfas-2015-0346>
- Stock, C. A., Alexander, M. A., Bond, N. A., Brander, K. M., Cheung, W. W., Curchitser, E. N., ... Werner, F. E. (2011). On the use of IPCC-class models to assess the impact of climate on living marine resources. *Progress in Oceanography*, 88(1–4), 1–27. <https://doi.org/10.1016/j.pocean.2010.09.001>
- Strogatz, S. H. (2014). *Nonlinear dynamics and chaos: With applications to physics, biology, chemistry, and engineering*. London, UK: Hachette UK.
- Tran, D., Andrews, M., & Ratilal, P. (2012). Probability distribution for energy of saturated broadband ocean acoustic transmission: Results from gulf of Maine 2006 experiment. *The Journal of the Acoustical Society of America*, 132(6), 3659–3672. <https://doi.org/10.1121/1.4763547>
- US-Senate. (2011). Hearing before the subcommittee on oceans, atmosphere, fisheries, and coast guard, one hundred twelfth congress, first session us senate committee on commerce, science, and transportation.
- Vitale, F., Borjesson, P., Svedäng, H., & Casini, M. (2008). The spatial distribution of cod (*Gadus morhua* L.) spawning grounds in the Kattegat, eastern north sea. *Fisheries Research*, 90(1–3), 36–44. <https://doi.org/10.1016/j.fishres.2007.09.023>

- Wang, D., Garcia, H., Huang, W., Tran, D. D., Jain, A. D., Yi, D. H., ... Ratilal, P. (2016). Vast assembly of vocal marine mammals from diverse species on fish spawning ground. *Nature*, 531(7594), 366. <https://doi.org/10.1038/nature16960>
- Wu, S. (1985). Phase structure and adhesion in polymer blends: A criterion for rubber toughening. *Polymer*, 26(12), 1855–1863. [https://doi.org/10.1016/0032-3861\(85\)90015-1](https://doi.org/10.1016/0032-3861(85)90015-1)
- Yi, D. H., Gong, Z., Jech, J. M., Ratilal, P., & Makris, N. C. (2018). Instantaneous 3D continental-shelf scale imaging of oceanic fish by multi-spectral resonance sensing reveals group behavior during spawning migration. *Remote Sensing*, 10(1), 108. <https://doi.org/10.3390/rs10010108>
- Zhang, W., Liu, Y., Ratilal, P., Cho, B., & Makris, N. C. (2017). Active nonlinear acoustic sensing of an object with sum or difference frequency fields. *Remote Sensing*, 9(9), 954. <https://doi.org/10.3390/rs9090954>

SUPPORTING INFORMATION

Additional supporting information may be found online in the Supporting Information section at the end of the article.

How to cite this article: Makris NC, Godø OR, Yi DH, et al. Instantaneous areal population density of entire Atlantic cod and herring spawning groups and group size distribution relative to total spawning population. *Fish Fish*. 2018;00: 1–13. <https://doi.org/10.1111/faf.12331>